Crosstalk between adjacent nanopores in a solid-state membrane array for multi-analyte high-throughput biomolecule detection

Muhammad Usman Raza,[1,2,3] Sajid Saleem,[4] Waqas Ali,[1,2,3,a)] and Samir M. Iqbal[1,2,3,5,6,b)]
[1]*Nano-Bio Lab, University of Texas at Arlington, Arlington, Texas 76019, USA*
[2]*Department of Electrical Engineering, University of Texas at Arlington, Arlington, Texas 76011, USA*
[3]*Nanotechnology Research Center, University of Texas at Arlington, Arlington, Texas 76019, USA*
[4]*Electronics and Power Engineering Department, National University of Sciences and Technology (NUST), H-12, Islamabad, Pakistan*
[5]*Department of Bioengineering, University of Texas at Arlington, Arlington, Texas 76010, USA*
[6]*Department of Urology, University of Texas Southwestern Medical Center at Dallas, Dallas, Texas 75390, USA*

(Received 19 March 2016; accepted 30 June 2016; published online 11 August 2016)

Single nanopores are used to detect a variety of biological molecules. The modulations in ionic current under applied bias across the nanopore contain important information about translocating species, thus providing single analyte detection. These systems are, however, challenged in practical situations where multiple analytes have to be detected at high throughput. This paper presents the analysis of a multi-nanopore system that can be used for the detection of analytes with high throughput. As a scalable model, two nanopores were simulated in a single solid-state membrane. The interactions of the electric fields at the mouths of the individual nanopores were analyzed. The data elucidated the electrostatic properties of the nanopores from a single membrane and provided a framework to calculate the −3 dB distance, akin to the Debye length, from one nanopore to the other. This distance was the minimum distance between the adjacent nanopores such that their individual electric fields did not significantly interact with one another. The results can help in the optimal experimental design to construct solid-state nanopore arrays for any given nanopore size and applied bias. *Published by AIP Publishing.*
[http://dx.doi.org/10.1063/1.4958673]

I. INTRODUCTION

Certain diseases such as cancer can lead to severe complications and drastically reduced survival rates if not detected early. Early detection is the key in fight against cancer which killed about 574 743 people in the United States in 2010 (or 186 deaths per 100 000 population) as shown by the data from Centers for Disease Control and Prevention.[1] These trends have not improved for many years. The survival rate of patients affected with cancer improve dramatically when diagnosis is made early in the disease life cycle.

The clinical symptoms of cancer do not show up until it has reached an advanced stage. Little can be done to contain or eliminate it then. The usual diagnostic tests leave much to be desired towards early and effective cancer detection. The need is for cheap, readily available and specific cancer diagnostic tools and methods.

In this paper, the problems associated with solid-state nanopore based detection of biomolecules are analyzed. A framework of nanopore arrays can sense multiple cancer biomarkers. The simulations lay foundations for rational design of electrically isolated nanopores in an array. The distance between adjacent nanopores, applied bias, and nanopore sizes define some basic design principles. In the end, the flow of an elliptical molecule is presented through a nanopore at two different adjacent nanopore distances. This demonstrates the utility of the solid-state nanopores in an array format for real-time sensing of protein molecules.

A. Solid-state nanopores

The nanopore biosensors are increasingly used for rapid and cost-effective detection of various biological analytes. The main reason for their emergence is the specific, label free and robust single molecule analysis capability. These can be used with varying functionalizations for the detection of multiple analytes.[2,3] There are two different kinds of nanopores. First are the biologically occurring α-hemolysin nanopores suspended in lipid bilayers made from *Staphylococcus aureus* which contains homoheptametric subunits leading to transmembrane channels of about 1.5 nm in diameter.[4–6] Second, the solid-state nanopores are made using silicon fabrication processes. Solid-state nanopores are relatively more robust and practical than the biological nanopores. Nanopores have been used to detect proteins, DNA and RNA complexes which may be linked to the detection of cancer.

Solid-state nanopores are fabricated by drilling holes in silicon nitride or silicon oxide membranes. Silicon nitride is generally preferred over silicon dioxide because it has low stress and remains intact even when its thickness is reduced to less than 10 nm.[7–9] However, the thickness of the

a) Present address: Intel Corporation, Santa Clara, CA 95054, USA.
b)Author to whom correspondence should be addressed. Electronic mail: SMIQBAL@uta.edu. Tel.: +1-817-272-0228. Fax: +1-817-272-7458. Present address: Department of Electrical Engineering 500 S. Cooper St #217, Box 19072, Arlington, TX 76019, USA.

membranes can further be reduced to a mere nanometer by using graphene.[10–12]

In the experiments, each nanopore chip is sandwiched between two containers filled with ionic solution. The two containers are separated by the nanopore in the membrane. The analyte to be detected is introduced in the appropriate side. Ag/AgCl electrodes are immersed in each container of ionic solution, and a voltage is applied across the nanopore. The analyte travels under the effect of bias through the solid-state nanopore. The ionic current through the nanopore gets disrupted when analytes pass through.[13] A large variety of biological molecules like DNA, RNA, disease biomarkers, and viruses have been detected with nanopores.[14–16] The side to which the analytes are introduced depends on the isoelectric point of the analyte,[17,18] the pH of the solution, and the polarity of the electrodes. The drop in the ionic current when the analyte passes through the nanopore results into the detection of the particular analyte.[19] This detection has been made specific by attaching ligands on the nanopore walls for a specific analyte under consideration.[2,20] The interaction of translocating species with nanopore surface grafted species results into characteristic negative peaks in the ionic current which makes detection of the specific analytes possible.[21] Single nanopore biosensors have many issues related to their practical implementations like baseline shifting, low throughput, and challenges in reproducible measurements.[22] On the measurements of nanopores, first, there is no self-referencing capability for the baseline current at any time when the analyte is passing through. Second, it cannot detect multiple analytes because the nanopore functionalization makes it specific to only one analyte. Third, the single nanopore sensor does not have the ability for differential operation that can be used to reduce noise for enhanced detection.[23] Fourth, if the single nanopore is blocked by a large molecule somehow,[24] it requires replacement of the nanopore, which means it lacks robustness. Last, and most importantly, the single nanopore biosensor has severely low throughput. This means that it takes a lot of time to process the millions of molecules in a sample looking for a few hundred copies of target biomolecule such as a cancer biomarker, especially at the early stages of the disease.

In order to circumvent problems associated with single nanopore technology, a framework of multiple nanopores made in the same membrane is presented here. Fig. 1 shows a model two-nanopore array.

B. Nanopore arrays

In a nanopore array, each nanopore has to be addressed with its own sensing electrodes, made on the membrane right close by. In line with this concept, the simulations consisted of two nanopores made in one membrane. When voltage bias was applied across the nanopores, a field was generated across the nanopores. This field resulted in the ionic current across the nanopores, moving the molecules through and ultimately causing pulses in the ionic current. The electrodes right next to the respective nanopores would detect the individual pulses in respective ionic currents. The measurements from each nanopore would thus provide quantitative pulse statistics related to the specific biomolecules. The system could detect multiple biomolecules at the same time and with throughput double than that through a single nanopore.

The problem of paramount importance in the nanopore array is that the adjacent nanopores have to be at a specific distance away from each other. If the distance is less, the electric fields from adjacent nanopores intersect with each other. This results in the ionic current drop at the metal electrodes to be affected by the adjacent nanopore currents leading to false results. Also, the distance between the nanopore mouth and the metal electrode has to be optimized so that the maximum detection is possible through the electrodes.

II. NANOPORE MODEL

A two-dimensional model was constructed to simulate the effects of adjacent nanopore electric fields on the translocation profiles. The nanopores were made in a silicon nitride membrane of 20 nm thickness. A 1 M KCl ionic solution was used in the model. It was contained in two containers of silicon nitride insulator separated in the middle by the silicon nitride membrane. The only paths between the two containers for the ionic current to flow were through the two nanopores. The depth of the 2D model was set at 5 nm (Fig. 2).

The materials used in the model consisted of silicon nitride with an electrical conductivity of 0 S/m, relative permittivity of 9.7, and density of 3100 kg/m^3. For 1 M KCl, the electrical conductivity was taken as 11 S/m and a relative

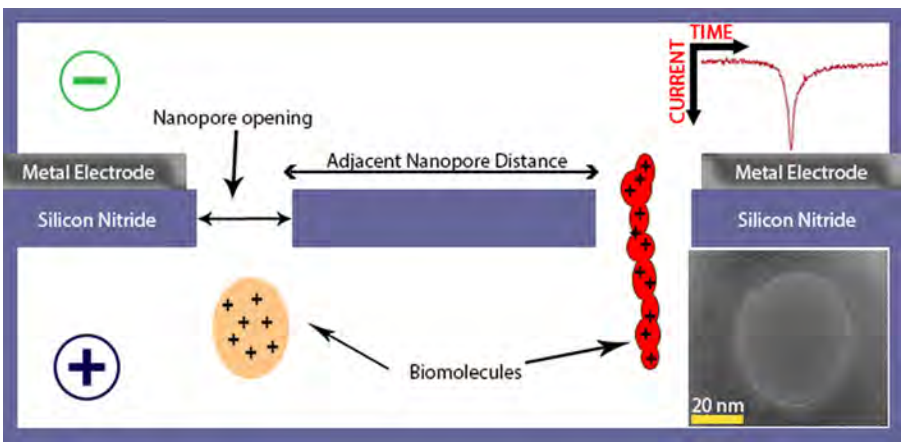

FIG. 1. A two-nanopore array. The biasing electrodes are shown in circles. These are immersed in the electrolyte solution. In the inset, the translocation time of the molecule is plotted against the translocation current through the nanopore. This shows that as the molecule passes through the nanopore, it results in a downward pulse in the current. The lower-right inset shows an actual 60 nm nanopore drilled in a silicon nitride membrane using transmission electron microscope.

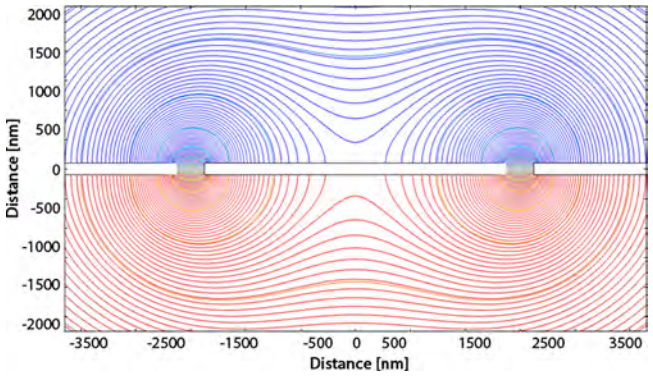

FIG. 2. The two-nanopore array model. The contour lines depict the electric field.

permittivity of 60.[25] The material KCl was assigned to be the ionic solution that was contained by the silicon nitride boundaries.

The COMSOL simulations used time-invariant electric currents physics model. The top and bottom plate was assigned as high potential and ground in this model, respectively. This resulted in the change in electric potential across the nanopore through the ionic solution (Fig. 3).

III. EXPERIMENTAL SETUP

In order to simulate the properties of a two nanopore array using the electric currents model, the DC bias was applied across a silicon nitride membrane. The ionic current flow was through the two adjacent nanopores. The simulations provided electric potential at the mouth of the nanopores to measure the best distance feasible between the two adjacent nanopores. It is important to note that the potential was the largest at the mouth of the nanopore where the molecules would exit the nanopore.

There were three variables in the nanopore array setup. These were the adjacent nanopore distance, the applied voltage bias, and the size of the nanopore. The three specific scenarios were simulated to measure their effects on electric potential through the two nanopores while keeping the other two factors constant. First, the distance between the adjacent nanopores was varied to find the optimum distance between two nanopores of certain size at fixed DC bias. Second, the effect of varying the DC bias applied across the nanopores was measured on the electric potential of adjacent

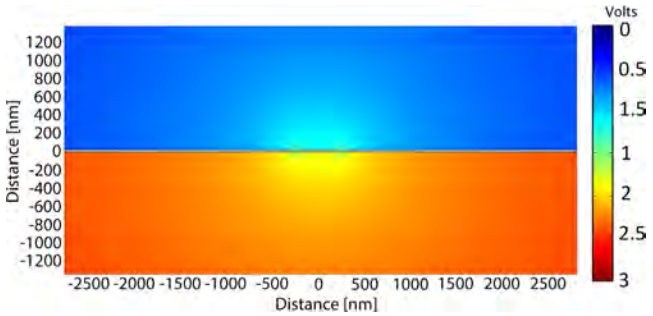

FIG. 3. A two nanopore array at 500 nm distance showing the interaction of the electric fields.

nanopores. Third, the effect of varying the size of the nanopores was found as it changed with the electric potential through two adjacent nanopores at fixed distance and fixed DC bias. These three parameters translated into the properties of measurement system that can be tailored to design for optimum results.

IV. RESULTS

The results of the simulations were plotted to get the best possible distance between the nanopores. At the end of each simulation and once equilibrium was achieved, the system snapshot was taken (Fig. 4).

A. Variation in nanopore distance

Figure 4 shows two cases, out of many (Fig. 5), with inter-nanopore distances of 1000 nm and 4000 nm. As can be seen in Fig. 4(a), the electric fields of two nanopores intercept each other in the ionic solution, while the ionic solution is passing through the nanopore. The direction of flow of anions and cations in the 1 M KCl solution is opposite to one another as these pass though the nanopore. This is due to the net charge on the individual K^+ and Cl^- ions in the solution and the effect of electric field on them. The net movement of charge through the nanopores created an ionic current flowing through these nanopores. The nanopores provided resistance to the flow of ionic current due to the small size of the opening. This resulted in the maximum potential drop across the nanopores, hence leading to the maximum magnitude of electric field at the nanopore mouth.

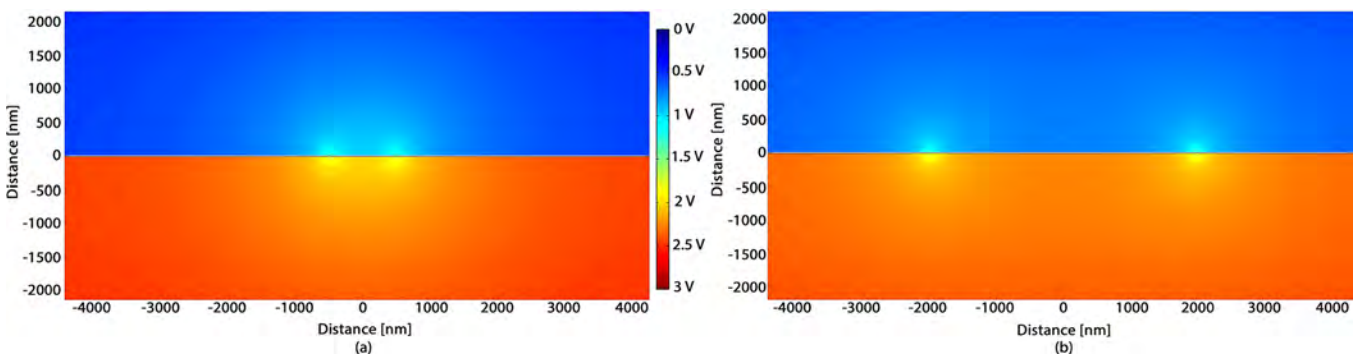

FIG. 4. The nanopores separated by (a) 1000 nm and (b) 4000 nm.

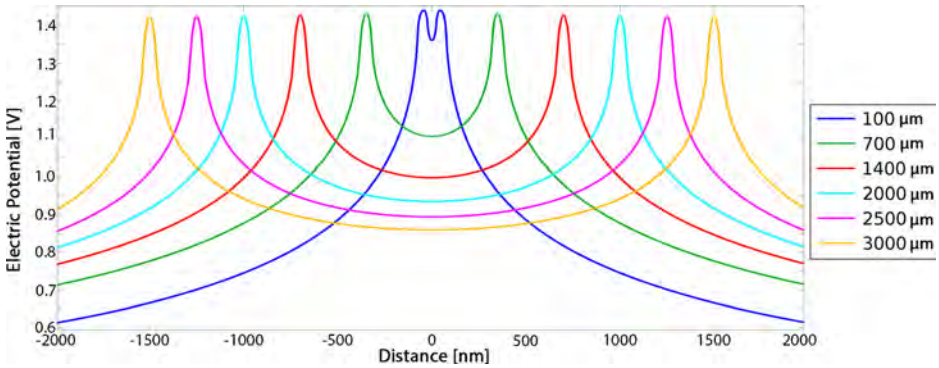

FIG. 5. The electric potential at the adjacent nanopores separated by increasing distance show that as the adjacent nanopore distance increases, the electric potential at the middle of the two nanopores also decreases.

Fig. 5 shows the effect of the variation in adjacent nanopore distance on the electric potential at the DC bias of 3 V and at the nanopore size of 50 nm. As the adjacent nanopore distance increased, the electric potential between the nanopores decreased significantly. The peak electric potential was thus at the mouth of the nanopore, and it degraded significantly as the distance from the mouth of the nanopore increased. For two adjacent nanopores to be independent of the electric fields of each other, the amplitude of electric potential should drop by at least −3 dB at the adjacent nanopore midpoint. So, if the peak amplitude is V_o, then the −3 dB amplitude of the electric potential should be less than $0.709V_o$. The simulations showed that at an adjacent nanopore distance of 2 μm or higher, the value of the electric potential at the adjacent nanopore midpoint was less than −3 dB value of peak electric potential at the mouth of the nanopore which is also the Debye length. This distance was enough for the adjacent nanopore electric fields to not interfere with each other.

B. Variation in DC bias

The electric potential interference change was linear at all points of interest when the distance between 50 nm nanopores was kept at 5000 nm and the DC bias across the nanopore was reduced from 5 V to 1 V (Figs. 6 and 7). From the data, it can be seen that the required adjacent nanopore distance is less for systems with lower applied bias, and the rate of change of applied bias at the center of the nanopore is the highest (Fig. 8(a)). This shows that for optimum detection of

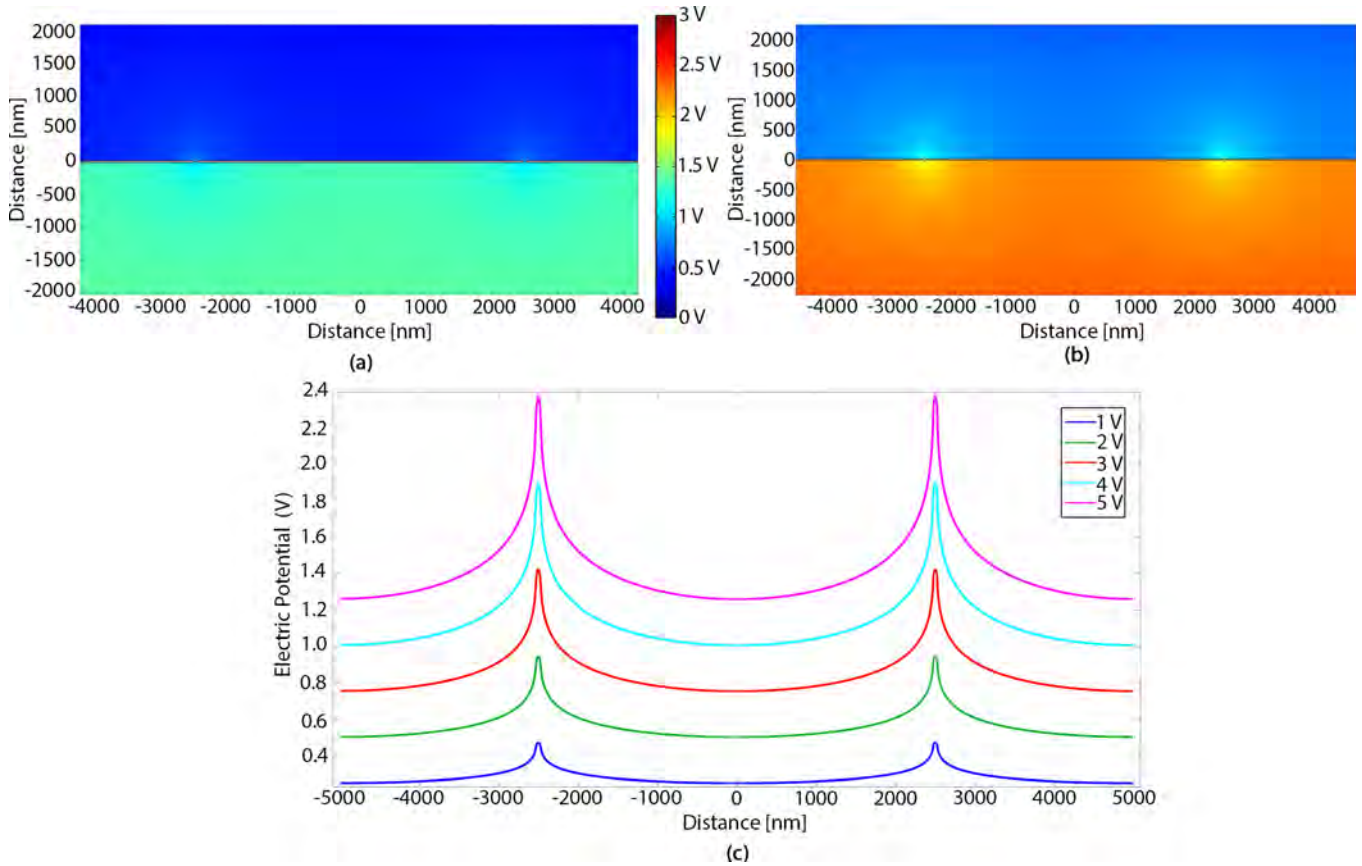

FIG. 6. The field at DC bias of (a) 2 V and (b) 3 V. (c) The change in electric potential as the DC Bias is varied. This shows that as the DC bias is reduced, the adjacent nanopore distance required to minimize crosstalk also becomes smaller. AA′ and BB′ slices are explored further to analyze the change in the electric potential with respect to the applied bias in later text.

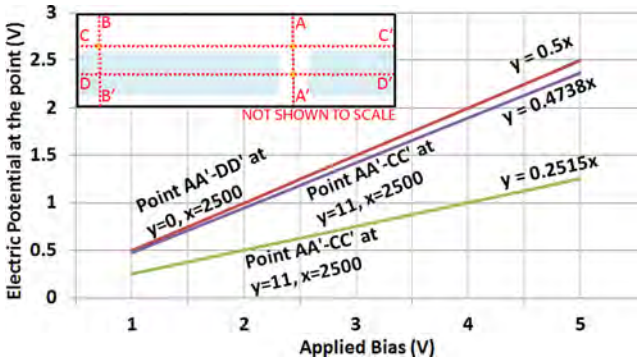

FIG. 7. The plot shows the linear behavior of the electric potential at various points in the ionic solution. The rate of change of applied bias is largest at the center of the nanopore and reduces at points away from the center of the nanopore.

the translocating biomolecule through the nanopore, electrodes should be placed at the center of the nanopore sandwiched inside the nanopore membrane. Sensitivity of the electrodes will be thus maximum if placed in the middle of the nanopore which is experimentally challenging.

In line with the limitations of actual fabrication, the electrodes were placed at the mouth of the nanopore where the rate of change was relatively lower. The y-component of electric field was also the highest at the center of the nanopore (Fig. 8(b)). This shows that the pull on the biomolecule would be the highest at the center and would decrease as it moves outwards towards the mouth of the nanopore. As a consequence, the translocation acceleration of the biomolecule will be the highest at the center of the nanopore. This shows that even a distance of less than the required 2 μm would be enough between adjacent nanopores at a bias of 1 V, which is in the range of voltages employed in the nanopore experiments.[26]

As shown in Fig. 1, the nanopore sensors are used to selectively detect biomolecules passing through the nanopore. These biomolecules can behave as anions or cations when suspended in solutions of different pH according to their isoelectric points. The net charge on the individual molecules determines whether the target biomolecule will be suspended on the negative or positive side of the nanopore. As the biomolecules have complex structures, if the electric fields at the mouth of the nanopores are high, the molecules start to loose their shape and characteristics.[21] This can result in flawed experimental results. The higher the DC bias, more field is felt by the biomolecule to translocate through the nanopore. This behaves as an accelerating force on the biomolecule and leads it to pass through the nanopore in less time leading to less interaction of the biomolecule with the nanopore or the nanopore grafted ligands. This high acceleration is thus undesirable in nanopore experiments as it may result in the loss of selective biomolecule detection.

The DC bias across the nanopore membranes thus has to adjust to values that lead to translocation of these biomolecules across the nanopore without disrupting their molecular structures and without interfering with sub-molecular forces. That is one of the reasons of using very low bias values in actual nanopore experiments, down to about 100 mV in some experiments.

C. Variation in nanopore size

The third variable was the nanopore size, varied while keeping the adjacent nanopore distance and the applied DC bias constant. The need for change in nanopore size is dictated by the fact that the biomolecules used in the experiments (as shown in Fig. 1) are of varying shapes and sizes. If the biomolecule size is much smaller than the size of the nanopore, the biomolecule may not significantly block the flow of ionic current through the nanopore. This would result in nonspecific and insignificant drops in ionic current during translocation. On the other hand, if the size of the biomolecule is larger than that of the nanopore, it would cause permanent blockage or may result in molecule deformation and loss of molecular shape, structure, and functionality.

The detection of specific biomolecules requires that the nanopore walls are functionalized with specific ligands that attach selectively with the translocating biomolecules of interest. Larger nanopore may result in lack of significant interactions between the translocating biomolecules and the ligands functionalized on the walls of the nanopore. Therefore, the size of the nanopore has to be designed based on the size of the translocating species and the layer thickness of ligands.

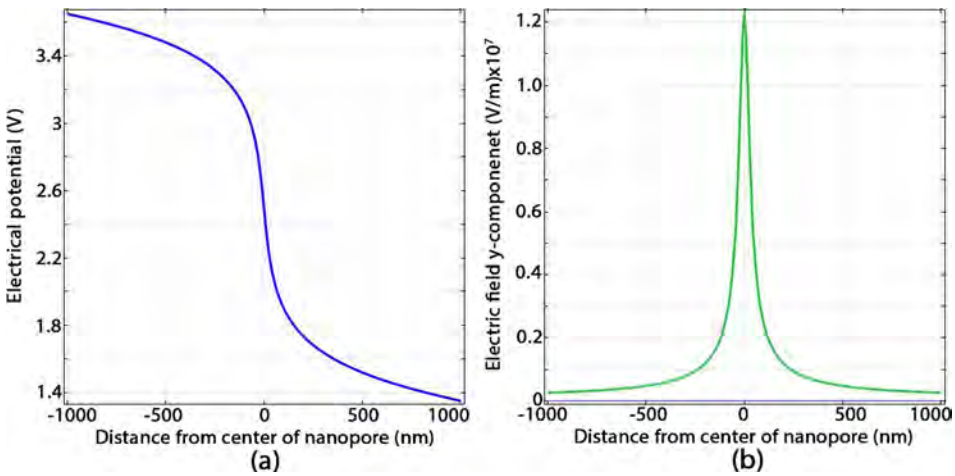

FIG. 8. Plots show the relationship of (a) electric potential and (b) the y-component of the electric field along the line AA′ (line AA′ is shown in inset of Fig. 7).

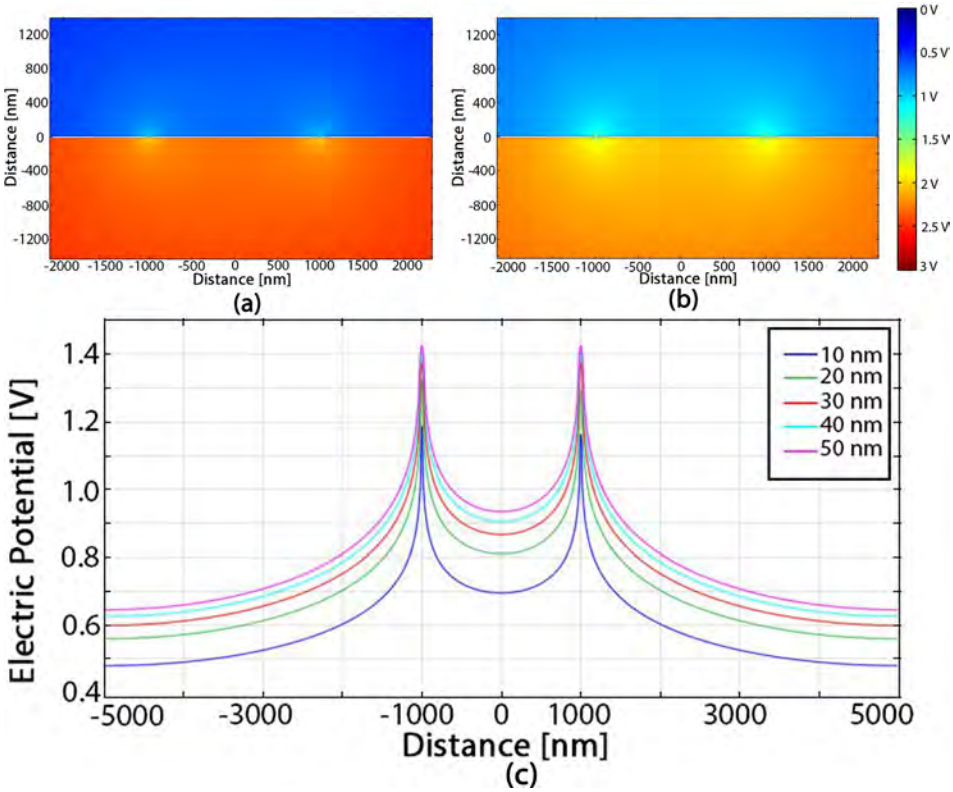

FIG. 9. The field with nanopore diameter of (a) 10 nm and (b) 50 nm. (c) The variations in electric potential with the nanopore diameters show that the larger diameter nanopores require more separation between adjacent nanopores.

Fig. 9 shows the electric potential between adjacent nanopores as the nanopore sizes were varied, but the adjacent nanopore distance was kept constant at 2000 nm and DC bias was set at 3 V. These data further elucidate that a nanopore size of 50 nm is good enough when the next nanopore is just 2 μm away. The 2 μm inter-nanopore distance at 3 V bias provides smooth operation of the nanopore array biosensor without adjacent nanopore crosstalk. It is thus easy to decide the configurations for a multi-nanopore multi-analyte detection scheme.

V. BIOMOLECULE TRANSLOCATION THROUGH THE NANOPORE

To further validate the preceding results with a biomolecule, simulation was also done with an elliptically shaped

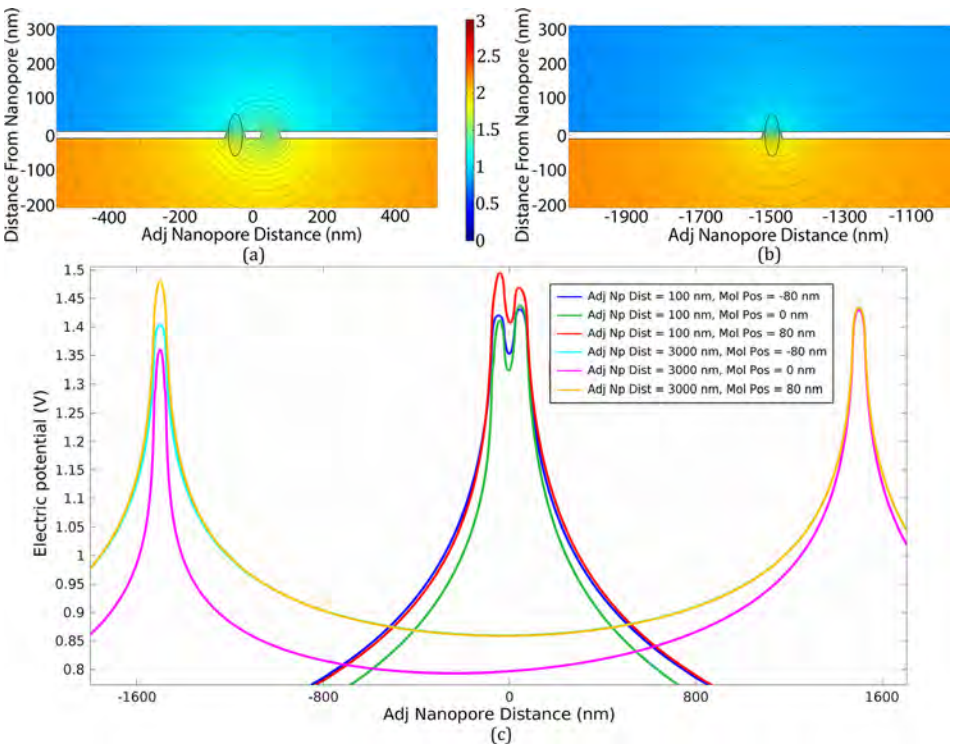

FIG. 10. (a) and (b) An elliptical molecule translocating through the nanopores. The adjacent nanopore distance in (a) is 100 nm and in (b) is 3000 nm. The molecule is right at the nanopore center in both (a) and (b). The contour lines represent the electric potential. (c) The electric potential at the mouth of the nanopore.

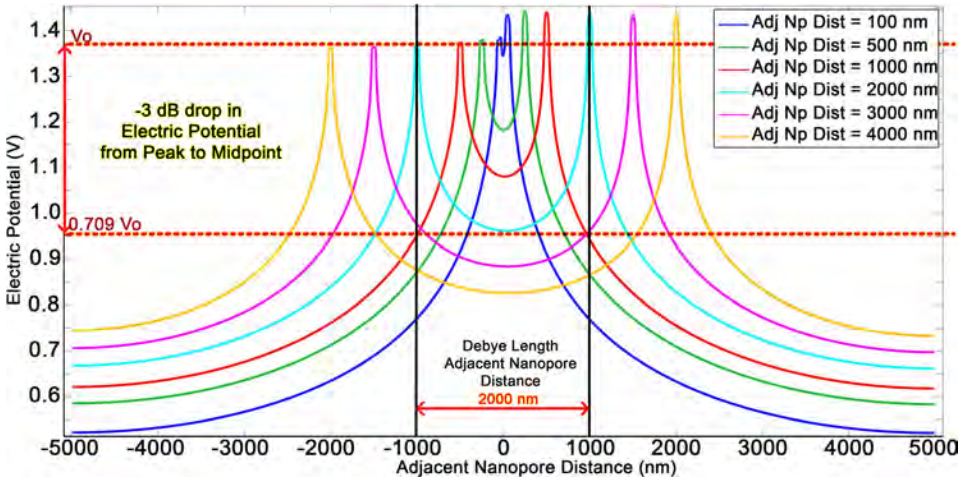

FIG. 11. The case of voltage at the mouth of the nanopore as the elliptical molecule passes through the nanopore and is at a point 80 nm past the center of the nanopore. We clearly see that the Debye length is 2000 nm as the −3 dB drop in electric potential between the peak and midpoint is $0.709\,V_o$.

protein. Epidermal growth factor receptor (EGFR) is a cell surface receptor that is overexpressed in many cancers. The radius of EGFR is about 20 nm and it is 40 nm long. The molecule is negatively charged at neutral pH, so a charge number of −1 was used to simulate the negatively charged molecule. The applied bias was 3 V and the nanopore diameter was 50 nm. For this simulation, two distances (between adjacent nanopores) were used. First adjacent nanopore distance was 100 nm which was less than the Debye length. The second adjacent nanopore distance used was 3000 nm which was more than the minimum distance for these conditions.

Fig. 10(a) shows the electric potential contours at 100 nm, while the molecule is passing through the nanopore on the left. It can be seen that the nanopore on the right is so close that it is significantly affected by the electrical

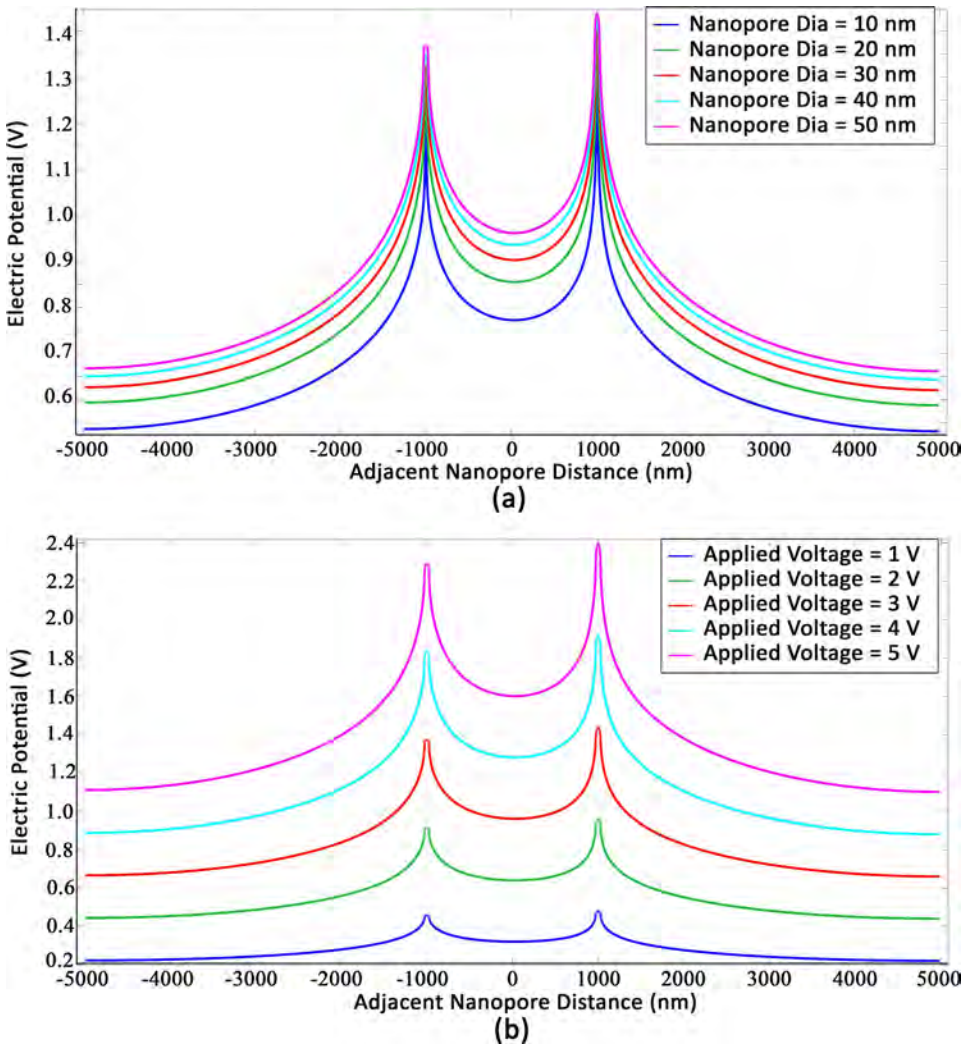

FIG. 12. (a) Change in nanopore diameter when the applied voltage is constant at 3 V, the adjacent nanopore distance is 2000 nm and the molecule is positioned 80 nm from the center of the nanopore. The voltage drop is for the mouth of the nanopore as the elliptical molecule passes through the nanopore. (b) The case of change in applied voltage as the nanopore diameter is kept at 50 nm and the adjacent nanopore distance is kept at 2000 nm and the molecule is again at 80 nm from the center of the nanopore.

interference from the changes in electric field from the adjacent nanopore. This shows that at a distance less than Debye length, 100 nm distance in this instance, the results may be false and nonspecific. The adjacent nanopore distance of 3000 nm, which is much more than the Debye length of 2000 nm, shows no electric potential distortion when the molecule passed through the left nanopore (Fig. 10(b)).

Fig. 10(c) shows that at an adjacent nanopore distance of 100 nm, when the molecule passes through the left nanopore, there is significant change in the electric potential at the mouth of the nanopore as well. However, there is absolutely no change in the electric potential at the right nanopore when it is 3000 nm apart. So in this case there will be no false results in the experiments.

The data show that a protein would be difficult to detect and give nonspecific results if the design constraints are not met. Hence, a nanopore with an adjacent nanopore more than Debye length away would result in negligible crosstalk and true molecule detection. Calculating the Debye length, i.e., the −3 dB drop in voltage from the peak to the midpoint is done in Fig. 11. It shows clearly the case of a translocating molecule at 80 nm from the nanopore. The Debye length has been calculated by calculating the length at which the midpoint voltage is 0.709 of the peak voltage. It is clearly shown for a case when the nanopore diameter is 50 nm and the applied voltage is 3 V, the Debye length is 2000 nm between the adjacent nanopores. At 2000 nm adjacent nanopore distance V_o is 1.37 V at the mouth of the nanopore with the translocating molecule. At midpoint of the two nanopores, the voltage is 0.97 V. This turns out to be $0.709V_o$ which is what we require. So, we conclude that the Debye length in this case is 2000 nm for adjacent nanopore distance. Finally, for the construction of the nanopore array system, for 3 V applied voltage, the adjacent nanopores should be more than 2000 nm apart.

Another important aspect of a multiple nanopore array is to see how the voltage drop from the molecule translocation changes at variable voltages and for variable nanopore sizes. The relationship of molecular translocation to nanopore diameter and applied voltage is depicted in Fig. 12, where the adjacent nanopore distance has been kept at 2000 nm. It is clear that the distance between adjacent nanopore has to be increased if we increase either the nanopore diameter or the applied voltage across the nanopore.

VI. CONCLUSIONS

Nanopore arrays have the potential to build more robust, faster, and highly selective molecular sensors. The throughput of the currently used single nanopore devices can be increased manifold if these were employed in array formats. With differential operation, noises can be subtracted from the experimental results leading to more sensitive detection of biomolecules. However, nanopore arrays bring forward a new set of design challenges. The simulations presented can guide fabrication towards optimum distance between two adjacent nanopores for them to function relatively independent of each other. It is also established that the nanopore array devices need electrodes at the mouth of the nanopores for differential measurements unlike conventional nanopores. The simulations show that the adjacent nanopore fabrication must be done while catering to the size and electrical characteristics of the biomolecule being investigated. The size of the nanopore and the applied bias have to be varied depending on the biomolecule. In short, all parameters have to be evaluated before fabrication of the nanopore array device as increase in applied bias or in nanopore size requires increase in the adjacent nanopore distance. The reduction in adjacent nanopore interference can open roadmap for multi-nanopore self-referencing systems that can go beyond current single nanopore frameworks.

ACKNOWLEDGMENTS

This work was supported by National Science Foundation, USA with grant number ECCS-1201878.

[1]S. L. Murphy, J. Q. Xu, and K. D. Kochanek, Natl. Vital Stat. Rep. **61**(4), 1 (2013).
[2]S. M. Iqbal, D. Akin, and R. Bashir, Nat. Nanotechnol. **2**(4), 243 (2007).
[3]H. He, R. H. Scheicher, R. Pandey, A. R. Rocha, S. Sanvito, A. Grigoriev, R. Ahuja, and S. P. Karna, J. Phys. Chem. C **112**(10), 3456 (2008).
[4]T. Osaki, H. Suzuki, B. Le Pioufle, and S. Takeuchi, Anal. Chem. **81**(24), 9866 (2009).
[5]L. Song, M. R. Hobaugh, C. Shustak, S. Cheley, H. Bayley, and J. E. Gouaux, Science **274**(5294), 1859 (1996).
[6]G. Maglia, M. R. Restrepo, E. Mikhailova, and H. Bayley, Proc. Natl. Acad. Sci. U.S.A. **105**(50), 19720 (2008).
[7]J. Li, D. Stein, C. McMullan, D. Branton, M. J. Aziz, and J. A. Golovchenko, Nature **412**(6843), 166 (2001).
[8]A. J. Storm, J. H. Chen, X. S. Ling, H. W. Zandbergen, and C. Dekker, Nat. Mater. **2**(8), 537 (2003).
[9]C. Dekker, Nat. Nanotechnol. **2**(4), 209 (2007).
[10]S. Garaj, W. Hubbard, A. Reina, J. Kong, D. Branton, and J. A. Golovchenko, Nature **467**(7312), 190 (2010).
[11]Z. S. Siwy and M. Davenport, Nat. Nanotechnol. **5**(10), 697 (2010).
[12]G. F. Schneider, S. W. Kowalczyk, V. E. Calado, G. Pandraud, H. W. Zandbergen, L. M. K. Vandersypen, and C. Dekker, Nano Lett. **10**(8), 3163 (2010).
[13]F. Haque, J. Li, H.-C. Wu, X.-J. Liang, and P. Guo, Nano Today **8**(1), 56 (2013).
[14]G. Maglia, A. J. Heron, D. Stoddart, D. Japrung, and H. Bayley, Methods Enzymol. **475**, 591 (2010).
[15]S. Howorka and Z. Siwy, Chem. Soc. Rev. **38**(8), 2360 (2009).
[16]R. Wei, T. G. Martin, U. Rant, and H. Dietz, Angew. Chem., Int. Ed. **124**(20), 4948 (2012).
[17]Y. Li, H.-H. Yang, Q.-H. You, Z.-X. Zhuang, and X.-R. Wang, Anal. Chem. **78**(1), 317 (2006).
[18]J.-R. Ku and P. Stroeve, Langmuir **20**(5), 2030 (2004).
[19]A. Meller, L. Nivon, and D. Branton, Phys. Rev. Lett. **86**(15), 3435 (2001).
[20]E. C. Yusko, J. M. Johnson, S. Majd, P. Prangkio, R. C. Rollings, J. Li, J. Yang, and M. Mayer, Nat. Nanotechnol. **6**(4), 253 (2011).
[21]M. A. I. Mahmood, W. Ali, A. Adnan, and S. M. Iqbal, J. Phys. Chem. B **118**(22), 5799 (2014).
[22]D. Wang, J. Bai, S.-w. Nam, H. Peng, R. Bruce, L. Gignac, M. Brink, E. Kratschmer, S. Rossnagel, P. S. Waggoner, K. Reuter, C. Wang, Y. Astier, V. Balagurusamy, B. Luan, Y. Kwark, E. Joseph, M. Guillorn, S. Polonsky, A. Royyuru, S. P. Rao, and G. A. Stolovitzky, Nanoscale **6**(15), 8900 (2014).
[23]D. Branton, D. W. Deamer, A. Marziali, H. Bayley, S. A. Benner, T. Butler, M. Di Ventra, S. Garaj, A. Hibbs, and X. Huang, Nat. Biotechnol. **26**(10), 1146 (2008).
[24]L. Movileanu, Trends Biotechnol. **27**(6), 333 (2009).
[25]PubChem Substance Database, 2015, Vol. 2015.
[26]W. Asghar, A. Ilyas, R. R. Deshmukh, S. Sumitsawan, R. B. Timmons, and S. M. Iqbal, Nanotechnology **22**(28), 285304 (2011).